PHYSICAL REVIEW B VOLUME 36, NUMBER 9 15 SEPTEMBER 1987-II

# Calculation of the barrier for oxygen incorporation into metal and metal-oxide surfaces

Peter Nordlander* and Maria Ronay
*IBM Thomas J. Watson Research Center, P.O. Box 218, Yorktown Heights, New York 10598*
(Received 24 April 1987)

Using a simple calculational scheme we investigate the potential barriers for oxygen incorporation into clean metals and metal-oxide surfaces. It is shown that the magnitude of the barrier depends on both the structure and the ability of the surface atoms to relax during the incorporation process. We apply the method to the first series of transition metals and their oxides and illustrate that trends in oxidation resistance depend on the magnitude of this barrier. We also show how defects at surfaces can reduce the barrier.

## I. INTRODUCTION

The oxidation of metal surfaces is a very common experience of daily life, and yet this well-known phenomenon of surface physics is relatively poorly understood. The reason for this is that the actual oxidation process of a metal involves several complicated steps. The oxygen molecules must dissociate, diffuse through an oxide layer, and finally react with the metal. These processes often occur at atmospheric pressure of oxygen. In addition to oxygen, the atmosphere contains several other types of molecules like water, which can also react with the metal and complicate the process. Furthermore, the relevant materials might have a high concentration of defects and even be noncrystalline. As a logical step towards the understanding of the corrosion of metals it was appropriate to study the initial oxidation of well-characterized metal surfaces in controlled atmospheres. Such systems have been studied experimentally and very valuable information and understanding has been extracted from such experiments.

Perhaps the key property of interest in the oxidation process is the rate with which an oxide layer grows. In order to relate the growth of the oxide layer to microscopic properties there is a need for kinetic models. Several models have been proposed and we will review only the ones that are relevant to this paper. For an extensive discussion see Ref. 1.

Mott's first theory[2] was proposed to explain the formation of protective oxide films on metals exposed to air near room temperature. According to this theory, for very thin films, the electrons will pass through the oxide layer by the quantum-mechanical tunnel effect as fast as they can be used up on the other side to form $O^{2-}$ ions, and the rate will be controlled by the rate of ion diffusion, i.e., $dL/dt \propto [L(t)]^{-1}$, where $L$ is oxide thickness and $t$ is time. Thus the oxide grows according to a parabolic growth law ($L \propto \sqrt{t}$). When the oxide becomes thicker, its growth is assumed to be limited by electron tunneling from the metal to the physisorbed oxygen molecules. The rate equation then takes the form, $dL/dt \propto \exp(-kL)$ which results in a logarithmic growth of the oxide, $L(t) \propto \log(t)$. Restrictions on this theory are that the temperature must be low enough to eliminate thermionic emission of electrons, but large enough to allow the thermal motion of ions.

In order to overcome the restrictions of the first theory, Mott proposed a second theory[3] which was repeated and expanded in what came to be known as the Cabrera-Mott theory.[4] According to this theory an equilibration of the metal Fermi level and the adsorbed oxygen level by electron transfer from metal to oxygen results in the establishment of a large positive uniform electric field across the oxide. This field is considered to lower the energy barrier $E_B$ for ion incorporation into the oxide. This theory gives an approximately inverse logarithmic[5] rate law, $1/L(t) \propto \log[t/L(t)^2]$.

While it is difficult to distinguish between logarithmic and inverse logarithmic growth laws, it seems, that only a few transition metals, (such as Ta, Cr, and Ni) obey Cabrera-Mott kinetics, while others (such as, for example, Cu) do not.[6]

We showed in a previous work[7] that the field develops only if there is a barrier to oxygen penetration on the surface, i.e., the oxygen ions must stay on the oxide surface to create a field. Since it is this barrier-induced field upon which the validity of the Cabrera-Mott theory depends, we estimated the magnitude of the barrier to oxygen penetration on metal and oxide surfaces using effective-medium theory and showed that the metals which oxidize by the Cabrera-Mott mechanism do have, or develop, a barrier on the surface to oxygen penetration, while the metals which do not oxidize by the Cabrera-Mott mechanism do not have a barrier to oxygen penetration on the surface to begin with or after the oxide has formed. We showed that the formation of NbO on an Nb surface dramatically increases the potential-energy barrier for oxygen incorporation, thereby evoking Cabrera-Mott kinetics. On the other hand, the formation of $Cu_2O$ on a Cu surface reduces the barrier to oxygen penetration. The lack of a surface barrier on oxidized copper then leads to parabolic kinetics. On Cr and Ni, both the metals and the oxides present a sizable barrier to oxygen penetration, thus the Cabrera-Mott mechanism is justified. We also showed how the height of the barrier is reduced by the relaxation of surface atoms, and related this relaxation to the second shear moduli of the metals and their respective oxides.[7]

 

In this paper we present the details of the method we used and discuss its limitations. We further apply the method to the complete first series of transition metals and their oxides and illustrate the importance of oxide structure for the magnitude of barrier heights. We confirm the role of the shear modulus in determining the magnitude of the relaxed barrier, and show how defects at surfaces can reduce the barrier. Finally, we will illustrate that trends in oxidation resistance depend on the magnitude of this barrier.

## II. THEORY

Even in the highly idealized situation, when a single oxygen molecule is considered outside a perfect metal, or metal oxide surface, it is not possible at present to model it exactly. Therefore we have used a simple approximate scheme, effective-medium theory,[8] to calculate the energy of an oxygen atom in the vicinity of a surface.

Effective-medium theory has previously been used to study equilibrium properties of hydrogen and oxygen chemisorption on transition metals.[9,10] It has been shown to provide quantitatively accurate results for chemisorption energies, heats of solution, bond lengths, adsorbate-adsorbate interaction effects, and adsorbate-vibrational properties for both hydrogen and oxygen on clean metal substrates. The incorporation of oxygen into Ni(111) has also been studied using effective-medium theory.[9] The authors showed that it was crucial to include lattice relaxation when calculating the potential barriers separating the chemisorption site from a subsurface site. The Ni lattice was modeled by a nearest-neighbor force model. Such a simple model does, however, not incorporate the proper elastic anisotropy of the substrate, and for a general description of barriers to oxygen incorporation on transition metals, it is necessary to describe the metal lattices in a better way. In the present calculation we will model the elastic response of the substrate using a lattice Green's-function technique, which properly accounts for the elastic properties of the substrate. In the present application we will consider oxygen on both clean metals and on oxides. The latter system represents a new type of application, and we will perform certain approximations that limit the accuracy of the approach. Since the starting point in our calculation will be an oxygen atom on a clean metal, we will start by reviewing effective-medium theory for the oxygen-metal system.[9]

The embedding energy of an oxygen atom into an inhomogeneous electron host of electron density $n_0(\mathbf{R})$ can be written as

$$\Delta E(\mathbf{R})=\Delta E_{\rm eff}^{\rm hom}(\bar{n}_0(\mathbf{R}))+\Delta E^{\rm hyb}(\mathbf{R})+\Delta E_v(\mathbf{R})+\Delta E_c(\mathbf{R}) . \quad (1)$$

The term $\Delta E_{\rm eff}^{\rm hom}(\bar{n}_0(\bar{R}))$ gives the dominant contribution to the interaction energy and describes the interaction between the oxygen and the valence electrons of the substrate. This term only depends on the average substrate valence-electron density, $\bar{n}_0(\mathbf{R})$, in the vicinity of the oxygen at the position $\mathbf{R}$. The theory prescribes that the averaging should be performed using the atom-induced electrostatic potential as a sampling function.[11] Due to the good screening properties of valence electrons, this is a localized quantity and the averaging is confined to a region within 2.5 a.u. around the oxygen atom. $\Delta E_{\rm eff}^{\rm hom}(n)$ is essentially equal to the embedding energy of an oxygen atom into a homogeneous electron gas of density $n$. Since this term is dominant in Eq. (1), it is proper to discuss the general features of this term. As a function of density $\Delta E_{\rm eff}^{\rm hom}$ has a shape characteristic of many reactive adsorbates. At low densities the energy goes down fairly steeply (we discuss an embedding energy so a negative value of $\Delta E$ means positive binding energy). This decrease in $\Delta E$ is due to the fact that the oxygen affinity is positive so it becomes energetically favorable for an electron to bind to the oxygen. At high densities on the other hand, the energy increases rapidly. This increase is due to the fact that the oxygen atom forms a negative ion with an almost inert electronic shell. The substrate electrons have to orthogonalize against this ion with a corresponding increase in kinetic energy. For this reason the phenomena is often referred to as kinetic energy repulsion.[11] Between these two regions there exists an optimum electron density for which the oxygen binds with a maximum energy. The terms $\Delta E_v(\mathbf{R})+\Delta E^{\rm hyb}(\mathbf{R})$ represent the first- and higher-order change in hybridization interaction between the oxygen and the one-electron states of the substrate. For a metal the dominant contribution comes from the interaction between the oxygen and the metal $d$ electrons. The term $\Delta E_c(\mathbf{R})$ is a short-range potential that describes the repulsive interaction between the oxygen atom and the substrate atom cores. The last three terms in Eq. (1) are relatively small correction terms to the $\Delta E_{\rm eff}^{\rm hom}$ term. While the correction terms are crucial for the understanding of trends in chemisorption energy, it has been found that many properties are well described by only retaining the $\Delta E_{\rm eff}^{\rm hom}$ term. For instance, the vibrational frequencies and the equilibrium bond distances of adsorbates at surfaces are accurately accounted for by this term.[10] The reason for this is that the correction terms vary only slowly with the position $\mathbf{R}$ of the adsorbate. The curvature of the potential-energy surface thus follows the electron density, a quantity which is known relatively accurately. In a calculation of the properties of hydrogen interstials in transition metals, it was also found that the trends in the heats of solution of hydrogen are very well accounted for by only the effective-medium term.[12] The reason for this is that the interstitial electron densities are so high that the effective-medium term totally dominates in Eq. (1). This is also the situation when an oxygen atom passes through a close-packed substrate layer. The distances between the oxygen and the substrate atoms get comparatively short and the substrate electron density around the oxygen atom becomes large. The interaction is then due to the kinetic energy repulsion. This repulsion is also the source of diffusion barriers in solids. For these reasons we will neglect the last three correction terms in Eq. (1) and only retain the effective-medium term in our expression for $\Delta E(\mathbf{R})$. We would like to emphasize that the above arguments only apply to oxygen incorporation

through the surface and not for diffusion along the surface. Since the absolute scale of the potential energy for oxygen atoms will depend on the values of the correction terms, and we focus on the barrier for oxygen moving from a chemisorption position into the nearest interstitial bulk position, we will assume that the energy zero is at the chemisorption position. The magnitude and shape of the barrier with respect to the chemisorption energy can then be calculated with the above method in a straightforward way.

In order to evaluate the $\Delta E_{\rm eff}^{\rm hom}$ term, the substrate electron density has to be known. We will simply assume that this quantity can be obtained by a linear superposition of atomic electron densities.[9,10] This might appear as a rather severe approximation, but since the oxygen atoms sample a substrate electron density within a region of 2.5 a.u. around its position, the average density does not depend on details of the valence-electron density. With this procedure the substrate electron density will directly depend on the positions $\{\mathbf{R}_j\}$ of the substrate atoms. We indicate this dependence by writing $n=n(\mathbf{R},\{\mathbf{R}_j\})$.

When the oxygen passes through a surface in its equilibrium configuration it will exert strong forces upon the substrate atoms in its vicinity. These forces will distort the lattice. The substrate atoms will relax so that the oxygen-substrate atom distances increase. This has the effect of reducing the oxygen-sampled electron density with a concomitant loss in kinetic energy repulsion. As has been shown in previous calculations,[9,7] it is crucial to include this relaxation when calculating the potential energy. The relaxation of substrate atoms requires energy since it involves a compression of the lattice, whereupon the distances between the substrate atoms get reduced, and the total energy gain is determined as a balance of the gain in kinetic energy repulsion and the energy cost of deforming the lattice. It is therefore important to model the substrate in a reasonable way. To describe the lattice deformation, we will use a linear-response approach that has been used previously to model the lattice distortions around hydrogen interstitials in transition metals.[12] The forces that the oxygen atom exerts on the substrate atoms can be calculated directly by differentiating the expression (1) for the total energy of the oxygen-substrate system with respect to the substrate atom coordinates:

$$\mathbf{F}(\mathbf{R}_i)=-\nabla_{\mathbf{R}_i}\Delta E_{\rm eff}^{\rm hom}(\bar{n}_0(\mathbf{R},\{\ldots,\mathbf{R}_i,\ldots\})) \ . \tag{2}$$

The response of the lattice can be described by the lattice Green's function,[13] $G_{\alpha\beta}(\mathbf{R},\mathbf{R}')$ which describes the displacement, $u^{\alpha}(\mathbf{R})$, in direction $\hat{\alpha}$ of a lattice atom at position $\mathbf{R}$ when a unit force is applied in direction $\hat{\beta}$ on a lattice atom at position $\mathbf{R}'$. For $\mathbf{R}'=\mathbf{R}$, the lattice Green's function $G$ describes the displacement of the same atom to which force is applied. Of all the different components of the Green's function this has the largest magnitude. For large separation between $\mathbf{R}$ and $\mathbf{R}'$, the Green's function decays only as $|\mathbf{R}-\mathbf{R}'|^{-1}$, and so for a proper description of the lattice deformation, it is important to include $G$ for a relatively large number of substrate atoms. In physical terms this means that the deformation energy of the lattice is distributed among a relatively large number of substrate atoms. The total displacement of the substrate atoms can be obtained by summing up all the displacements of substrate atoms generated by the applied forces. The final expression for the displacement of the substrate atoms reads

$$u^{\alpha}(\mathbf{R}_i)=\sum_{j,\beta}G_{\alpha\beta}(\mathbf{R}_i,\mathbf{R}_j)F^{\beta}(\mathbf{R}_j+\mathbf{u}(\mathbf{R}_j)) \ . \tag{3}$$

The energy stored in the lattice upon such a deformation is given by[12,14]

$$\Delta E_{\rm lat}=\tfrac{1}{2}\sum_i \mathbf{F}(\mathbf{R}_i+\mathbf{u}(\mathbf{R}_i))\mathbf{u}(\mathbf{R}_i) \ . \tag{4}$$

Ideally, one should use the exact lattice Green's function in Eq. (3), but unfortunately these quantities are generally not available. The lattice Green's function for the substrate is obtained using the continuum approximation for the lattice and can be expressed in terms of the elastic constants $c_{11}$, $c_{12}$, and $c_{44}$.[13,12] In this model the Green's function $G(\mathbf{R},\mathbf{R}')$ only depends on the relative distance, $\mathbf{R}-\mathbf{R}'$, and can be expressed as

$$G_{\alpha\beta}(\mathbf{R})=\int_{\rm BZ}g_{\alpha\beta}(\mathbf{k})\exp(i\mathbf{k}\cdot\mathbf{R}) \ , \tag{5}$$

where

$$g_{\alpha\beta}(\mathbf{k})=\frac{d\mathbf{k}}{(2\pi)^3}(c_{44}k^2)^{-1} \times\left[K_{\alpha}\delta_{\alpha\beta}-\gamma_0 K_{\alpha}K_{\beta}n_{\alpha}n_{\beta}\left[1+\gamma_0\sum_{i=1}^{3}K_i n_i^2\right]^{-1}\right]$$

and

$$K_{\alpha}=(1+\tau n_{\alpha}^2)^{-1} \ ,$$

$$\gamma_0=\frac{(c_{12}+c_{44})}{c_{44}} \ ,$$

$$\tau=\frac{(c_{11}-c_{12}-2c_{44})}{c_{44}} \ .$$

Here $n_{\alpha}$ are the direction cosines of $\mathbf{k}$. The integration has to be done numerically over the first Brillouin zone. We assume the Debye model which has a spherical Brillouin zone with a wave-vector cutoff equal to $k_D=(6\pi^2 n)^{1/3}$ where $n$ is the number of atoms per volume. The continuum model describes the lattice response fairly well. By comparing the calculated components of the continuum Green's function with the exact discrete lattice Green's function, we have found that the continuum model typically underestimates $G$ by up to 20%. Such a small discrepancy is certainly within the limits of the accuracy of the method. The calculated atomic distortions are fairly large, up to 15% for certain surfaces, so another source of error could be anharmonic effects in the lattice response. Such effects are expected to further increase the ability of the substrate to relax. We have also neglected chemical effects of the oxygen on the lattice, i.e., assumed that the substrate force constants are unaffected by the presence of the oxygen. This certainly is an approximation, since it is known that oxygen can modify surface force constants. For Ni,

for instance, it has been found, that the presence of an oxygen atom on the surface can reduce certain Ni-Ni force constants by up to 30%.[15] As will be shown below, however, the calculated barriers show very large variations for different substrates and structures. The trends and qualitative conclusions that we will present do not therefore depend on the details of our model for the substrate relaxation.

Using Eqs. (1)–(4), the lattice distortions and the potential energy for an oxygen outside the relaxed substrate can be calculated. Since the forces entering Eqs. (3) and (4) depend on the relaxations of the substrate atoms, the equations have to be iterated to self-consistency in the substrate atom displacements. To illustrate the effects of lattice relaxation we also perform calculations using only Eq. (1), and assume the lattice to be in its unrelaxed configuration. We have calculated the barriers by choosing minimal energy paths. The energy barrier presented is thus the lowest-energy barrier that separates a site outside the surface and a stable site inside the material. The paths connecting two such sites do, in general, turn in different directions to avoid certain substrate atoms. In the present paper we will focus our attention only on the magnitude of the potential barrier and will not present details about the diffusion paths.

In the schematic Fig. 1 we illustrate some basic concepts of the potential energy for an oxygen outside a metal. Far outside the surface, the energy starts at zero. As the surface is approached, the energy decreases. At a distance on the order of 2 a.u. outside the surface, there is a deep minimum in the potential energy. This minimum is the chemisorption position and we denote it as $E_{\text{chem}}$. As the oxygen moves further inwards, it encounters a potential barrier. This is the surface-incorporation barrier, and we denote it by $E_B$. Further inwards in the metal there is a minimum in the potential energy. This site corresponds to an interstitial site. The energy of an interstitial oxygen is denoted by $E_{\text{sorp}}$. The next barrier inwards is the diffusion barrier, which we denote by $E_D$. Provided the tops of the hills are at the same height, these energy barriers are related by a simple relation

$$E_B = E_D + (E_{\text{chem}} - E_{\text{sorp}}) \ . \tag{6}$$

If lattice relaxation is included, this relation has to be modified to include the difference in relaxation ability between the surface layer and the bulk layers. If the surface layer has a different structure from the bulk layers, the relation also has to be modified. The chemisorption energy is in general larger than the sorption energy because the electron density at an interstitial position is much larger than the optimal density, while at the surface the oxygen atom sits at the optimal density,[12] where the binding energy is maximal. This means that the barrier for surface incorporation is in general larger than the diffusion barrier. Note in Fig. 1 that the barrier height is given relative to the chemisorption well. All the barrier energies which we present were calculated relative to the chemisorption well.

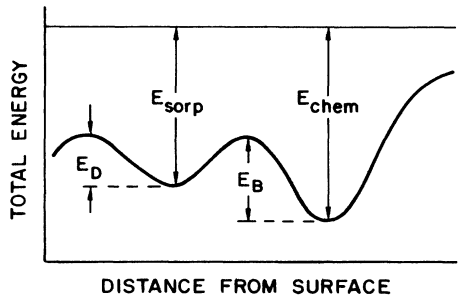


FIG. 1. Schematic illustration of the potential energy of an oxygen outside a metal. $E_{\text{chem}}$ is the energy at the chemisorption position, $E_B$ is the surface-incorporation barrier, $E_{\text{sorp}}$ is the energy at an interstitial site, and $E_D$ is the diffusion barrier.

## III. RESULTS AND DISCUSSION

It is our purpose in this paper to emphasize the importance of substrate structure and stiffness on the magnitude of the barrier to oxygen penetration. The closer packed the substrate atoms are, the larger is the electron gas density and thus the energy, $\Delta E_{\text{eff}}^{\text{hom}}$ of the oxygen embedded in the substrate, resulting in a larger barrier. Once a close-packed structure exists, however, whether the oxygen can penetrate or not, depends on the ability of the lattice to relax, and thus on its shear modulus.[7] These points can be illustrated very well on the first series of the transition metals and on some of their oxides, because these materials represent a rich variety of structures and strengths. Table I gives the structure, lattice parameter, and elastic constants of the first series of transition metals, while Table II gives the same data for some of their oxides.

As was mentioned in the Theory section, the main physical property that determines the height of the energy barrier is the substrate electron density. This electron density depends directly on the distances between the oxygen atom and the substrate atoms at the crossing point. As will be shown below, those distances depend directly on the structure of the substrate. In order to illustrate the simplest possible aspect of the importance of structure—the interatomic distances in the substrate—we will consider one type of structure and plot the calculated unrelaxed energy barriers for different materials versus the lattice constant. Since the rocksalt structure is a common structure among transition-metal monoxides, we show in Fig. 2 how the barrier energy changes with lattice constant in this series of transition-metal oxides. We can see in the figure that there is a strong correlation between the magnitude of the barrier and the lattice constant. A 10% increase in lattice constant reduces the unrelaxed barrier by a factor of almost $\frac{1}{3}$. This is a very strong effect, and it implies that structural effects are truly important. As we see from Fig. 2, it is the unrelaxed barrier which correlates most with the structure; the relaxed barrier seems to change less with the lattice constant.

The electron density at the crossing point is substantially reduced by the relaxation of the substrate atoms in the vicinity of the oxygen. Figure 3 shows the amount

TABLE I. Crystal structure, lattice constant, elastic constants, and the unrelaxed and relaxed barrier for the first series of transition metals. The elastic constants are given in units of $10^{12}$ dyn/cm$^2$ and with the exception of Mn were taken from *Point Defects in Metals I,* edited by G. Leibfried and N. Breuer (Springer, Berlin, 1980). The authors have not been able to find values for the elastic constants of Mn in the literature but estimated those simply by multiplying the elastic constants for Fe by the ratio of the bulk modulus for Mn and Fe. The lattice constants are given in Å.

| | Structure | $a$ | $c$ | $c_{11}$ | $c_{12}$ | $c_{44}$ | $E_B^0$ | $E_B^{rel}$ |
|---|---|---|---|---|---|---|---|---|
| Sc | hcp | 3.31 | 5.27 | 0.81 | 0.46 | 0.24 | 0.00 | 0.00 |
| Ti | hcp | 2.95 | 4.69 | 1.62 | 0.92 | 0.47 | 0.26 | 0.18 |
| V | bcc | 3.02 | | 2.29 | 1.19 | 0.43 | 1.47 | 0.91 |
| Cr | bcc | 2.88 | | 3.46 | 0.66 | 1.00 | 2.80 | 1.78 |
| Mn | cubic | 8.89 | | 0.80 | 0.45 | 0.40 | 2.70 | 0.85 |
| Fe | bcc | 2.87 | | 2.33 | 1.35 | 1.18 | 2.87 | 1.46 |
| Co | hcp | 2.51 | 4.07 | 3.07 | 1.65 | 0.76 | 4.22 | 1.74 |
| Ni | fcc | 3.52 | | 2.51 | 1.50 | 1.24 | 4.12 | 1.69 |
| Cu | fcc | 3.61 | | 1.69 | 1.22 | 0.75 | 2.80 | 0.88 |

of relaxation (unrelaxed barrier minus relaxed barrier as a percentage of the unrelaxed barrier) for the same transition-metal monoxides as a function of the second shear modulus $\frac{1}{2}(c_{11}-c_{12})$. The amount of relaxation decreases as the shear modulus increases. MnO shows relatively less relaxation than CoO in spite of the similarity of shear moduli; the reason for this is that MnO is a fairly open structure, as reflected by the large lattice constant. The forces between the oxygen atom and the MnO are therefore smaller, causing less relaxation of the substrate. We see that the amount of lattice relaxation varies between 50% and 70% of the magnitude of the unrelaxed barrier even within the same crystal structure. This is a significant effect, and immediately shows us, that in order to calculate the energy barriers for oxygen, we need to describe both the structure of the substrate and its elastic properties.

In Fig. 4(a) we show the unrelaxed and relaxed barriers for the first series of transition metals. The increase in the magnitude of the unrelaxed barrier towards the right of the Periodic Table is due to an increase of the interstitial electron density. This increase is due to both getting more electrons per atom and also to smaller lattice constants for the elements towards the noble metals. The relaxed barriers, however, show a much smaller variation along the 3*d* series. This is because the metals to the right are generally softer than the metals to the left, and can therefore relax more. As suggested in our previous work,[7] the magnitude of the relaxed barrier correlated best with the second shear modulus,

TABLE II. Crystal structure, lattice constant, elastic constants, and the unrelaxed and relaxed barrier for some oxides of the first series of transition metals. The lattice constants $a$ and $c$ are given in Å. The elastic constants are given in units of $10^{12}$ dyn/cm$^2$.

| | Structure | $a$ | $c$ | $c_{11}$ | $c_{12}$ | $c_{44}$ | $E_B^0$ | $E_B^{rel}$ |
|---|---|---|---|---|---|---|---|---|
| $Sc_2O_3$ | bixbyite | 9.84 | | 2.27[a] | 1.38[a] | 0.69[a] | 0.00 | 0.00 |
| TiO | rocksalt | 4.18 | | 4.00[b] | 1.00[b] | 1.00[b] | 4.78 | 2.35 |
| $TiO_2$ | rutile | 4.59 | 2.96 | 2.66[c] | 1.73[c] | 1.24[c] | 0.16 | 0.07 |
| VO | rocksalt | 4.06 | | 4.00[b] | 1.00[b] | 1.00[b] | 7.01 | 3.28 |
| $Cr_2O_3$ | corundum | 4.96 | 13.59 | 3.74[d] | 1.48[d] | 1.59[d] | 4.84 | 1.49 |
| MnO | rocksalt | 4.44 | | 2.27[e] | 1.16[e] | 0.78[e] | 2.58 | 0.97 |
| $Mn_2O_3$ | bixbyite | 9.41 | | 2.27[f] | 1.16[f] | 0.78[f] | 0.05 | 0.01 |
| FeO | rocksalt | 4.31 | | 2.17[e] | 1.21[e] | 0.46[e] | 3.99 | 1.18 |
| $Fe_3O_4$ | spinel | 8.39 | | 2.17[g] | 1.21[g] | 0.46[g] | 0.49 | 0.21 |
| CoO | rocksalt | 4.27 | | 2.60[e] | 1.45[e] | 0.80[e] | 4.62 | 1.51 |
| $Co_3O_4$ | spinel | 8.09 | | 2.60[h] | 1.45[h] | 0.80[h] | 1.21 | 0.60 |
| NiO | rocksalt | 4.17 | | 2.25[i] | 0.95[i] | 1.10[i] | 5.58 | 1.79 |
| $Cu_2O$ | $Cu_2O$ | 3.61 | | 1.21[e] | 1.05[e] | 0.12[e] | 0.16 | 0.03 |

[a]Values for $Y_2O_3$ were used.
[b]Values for NbO were used. See Ref. 7.
[c]From J. B. Wachtman, Jr., W. E. Tefft, and D. G. Lam, Jr., J. Res. Natl. Bur. Stand **66a**, 465 (1962).
[d]From H. L. Alberts and J. C. A. Boeyens, J. Magn. Magn. Mater. **2**, 327 (1976).
[e]From *Landolt-Börnstein* (Springer, Berlin, 1984), Vol. III/18, pp. 14 and 15.
[f]Values for MnO were used.
[g]Values for FeO were used.
[h]Values for CoO were assumed.
[i]From *Landolt-Börnstein* (Springer, Berlin, 1979), Vol. III/11, p. 28.

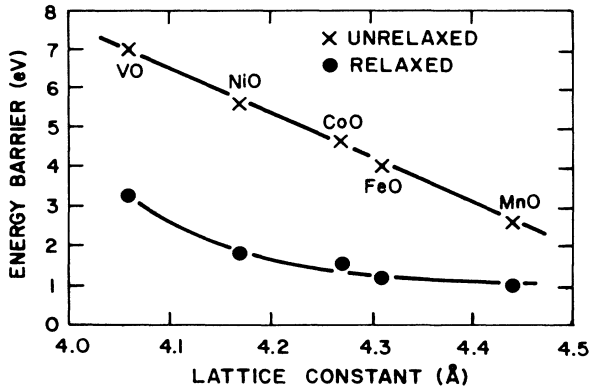


FIG. 2. The change of barrier energy with lattice constant on transition-metal oxides with the rocksalt structure. The top curve shows the unrelaxed barrier, the bottom curve the relaxed barrier.

$\frac{1}{2}(c_{11}-c_{12})$. We show this in Fig. 4(b) for the $3d$ series excepting Ni and Cu, where the relevant quantity is $\frac{1}{3}(c_{11}-c_{12}+c_{44})$,[16] and it is clear, that the trend in the magnitude of the relaxed barrier follows the trend of the shear moduli. This correlation indicates that for metals the stiffness is more important than the structure in determining the energy barriers. The reason for this is that in metals the structure varies less than the elastic constants, which vary more than a factor of 4 among the $3d$ metals.

Figure 5 shows the unrelaxed and relaxed barriers on, what we believe—arguably—are the oxides which form on the surface of the first series of transition metals, when oxidation takes place near room temperature, and under low partial pressures of oxygen. While it is not only the barrier to oxygen penetration which can provide the rate limiting step in oxidation, on some very neutral oxides such as $TiO_2$, the rate limiting step may be the dissociation of oxygen molecules; in the case of other oxides, which are very good insulators, such as $Al_2O_3$, the rate-limiting step may be electron tunneling. Nevertheless we shall see that the barrier to oxygen penetration does determine the trend in oxidation resistance. Figure 5 shows how penetrable the oxides on these transition metals are to oxygen, and this seems to

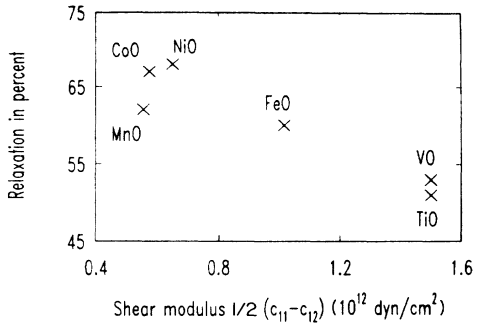


FIG. 3. The amount of relaxation as a function of the second shear modulus for transition-metal oxides with the rocksalt structure.

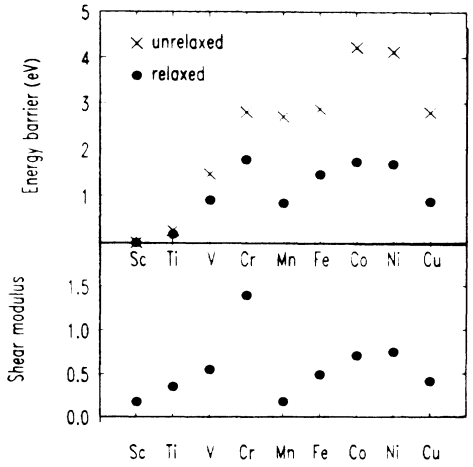


FIG. 4. (a) The unrelaxed and relaxed barriers for the first series of transition metals; (b) the magnitude of the second shear modulus for the first series of transition metals. Shear modulus is in $10^{12}$ dyn/cm$^2$. For further details see the text.

give the same trend as oxidation resistance determined by experiment. The minima in the curve show negligible barriers to oxygen penetration on the oxide and this coincides with little resistance to oxidation in the metal. Scandium oxidizes very easily. Oxygen incorporation into manganese is extensive already at 78 K;[17] actually manganese oxidizes so readily, that manganese films are used as corrosion indicators.[18] On an iron surface, under the oxidation conditions of interest here, the structure of the oxide on the surface appears to lie between that for $\gamma$-$Fe_2O_3$ and $Fe_3O_4$.[19] Since $\gamma$-$Fe_2O_3$ can be conceived as a spinel structure with vacant positions in the metal lattice,[20] and $Fe_3O_4$ is that very spinel, for sake of simplicity we calculated the barrier for $Fe_3O_4$. The relatively low barrier is in agreement with the well-known propensity of iron to oxidation. The high points on the curve represent a great resistance to oxygen penetration in the oxide and thus we expect a good resistance to oxidation. The oxidation resistance of titanium, chromium, and nickel are well known. Perhaps it is a less-known fact, that vanadium is also extremely resistant to oxidation at room temperature.[21] What these re-

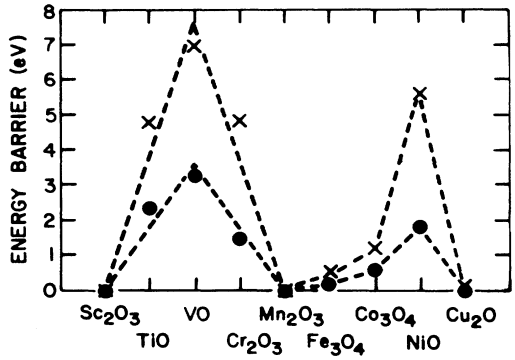


FIG. 5. The unrelaxed and relaxed barriers on the oxides of the first series of transition metals. The magnitude of the relaxed barrier indicates the trend in oxidation resistance.

sults confirm is that oxidation resistance requires protective oxide films, protective not in the sense emphasized before, that for one reason or another they stop growing, but protective in the sense that they are difficult to penetrate by oxygen. It can also be seen in Fig. 5 that the variation in the magnitude of the relaxed barriers closely follows the variation of the unrelaxed barriers. This means, that for oxides the main physical quantity that determines the oxidation resistance is the structure of the oxide. Even though lattice relaxation reduces the energy barriers by as much as 70%, the trend in oxidation resistance that emerges from Fig. 5 is the result of structural effects. This is in contrast with the behavior of the clean metals. The reason for this difference is that in the oxides there is an enormous variation in structure, while the elastic constants vary considerably less, only by a factor of 2.

As has been mentioned above, the structure of the oxide surface plays an absolutely crucial role in the magnitude of the barriers. This is perhaps best exemplified by a comparison of the energy barrier for oxides of the same transition metals which form a variety of structures. As seen from Table II, the relaxed barrier for $TiO_2$ is 0.07 eV, while for TiO it is 2.35 eV. For $Mn_2O_3$ the barrier is 0.01 eV, but for MnO the barrier is 0.97 eV. For $Co_3O_4$ the barrier is only 0.60 eV, while for CoO the barrier is 1.51 eV. These variations in barrier energy are due to structural effects. The rocksalt structure is very homogeneous and closepacked, but in the rutile, bixbyite, and spinel structures there are open channels, through which the oxygen can diffuse easily. The bixbyite structure for example can be envisioned as a fluorite structure with ordered vacancies. The oxygen atom can migrate through these vacancies without having to penetrate the high electron density regions of the substrate. It is such ordered vacancies which open up the "channels."

To further illustrate the importance of defects and inhomogeneities in the oxide structure, we have calculated the potential energy for an oxygen atom outside a perfect NbO(111) and an NbO(111) with a vacancy in the third layer. The result is shown in Fig. 6. There is a very large difference between the two barriers. For the perfect (111) surface, the barrier is 4 eV, while in the presence of a vacancy, it is only 1.2 eV. The vacancy thus reduces the barrier dramatically.

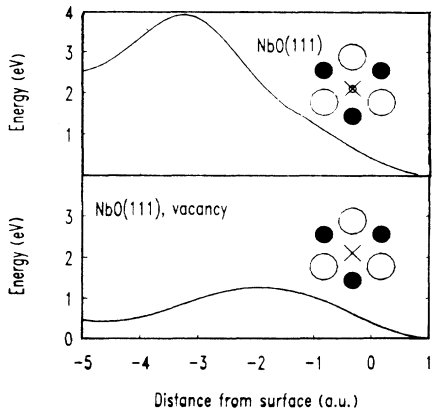


FIG. 6. The barrier on (a) a perfect NbO(111) surface, and, (b) on an NbO(111) surface with a vacancy in the third layer.

## IV. CONCLUSIONS

Using a simple calculational scheme we have calculated the potential energy for an oxygen atom in the vicinity of a metal and metal oxide surface. We have shown, that in general there is a large potential energy barrier separating the chemisorbed state from a subsurface position. The physical mechanisms underlying the existence of this barrier have been elucidated and it has been shown that the energy barrier results from the repulsive forces due to kinetic energy orthogonalization between the penetrating oxygen atom and the substrate valence electrons. We have demonstrated that these repulsive forces can be significantly reduced by a local distortion of the substrate atoms around the oxygen atom. The magnitude of the barrier is thus obtained as a balance in energy due to the decrease in kinetic energy repulsion when the lattice relaxes, and the energy cost of deforming the lattice. The model contains no adjustable parameters and expresses the potential energy of the oxygen-substrate system in terms of the electronic structure and the elastic constants of the substrate.

In an application to the oxidation of transition metals, the model has been shown to provide results that compare very well with experimental findings. We have demonstrated that the energy barriers for oxygen on a transition-metal oxide surface can be very different from the barrier on the corresponding clean metal surface. This has the important consequence that a metal's resistance to oxidation can be improved dramatically by the formation of an oxide layer. For transition-metal oxides we have found that the barrier for oxygen penetration depends very much on the structure and the stoichiometry of the oxide. We have shown that, for instance, the monoxides, which crystallize in the rocksalt structure, show very large energy barriers for oxygen incorporation. The experimentally observed trends in oxidation resistance of transition metals are well accounted for in terms of the structures of the oxides. We have shown that defects in the oxide structures can open up diffusion paths with much lower activation energies than the perfect oxide structures.

We have further demonstrated that the energy barriers are significantly reduced by lattice relaxation, and that if this effect is not properly taken into account, there is no hope for even a rough quantitative understanding of the barriers for oxygen penetration through surfaces. In particular for clean metals, where the lattices are comparatively soft, and lattice relaxation is therefore large, the trends in the magnitude of the barrier to oxygen incorporation can be directly correlated to the stiffness of the metal lattice.

The proposed calculational scheme is easily generalizable to other important incorporation phenomena, like Cl and F etching of metallic substrates, and we can expect the same qualitative conclusions about the importance of the substrate structure and stiffness to apply also in these situations.

*Present address: The Center for Atomic and Molecular Physics at Surfaces, Department of Physics and Astronomy, Vanderbilt University, Nashville, TN 37235.

[1]A. T. Fromhold, Jr., *Theory of Metal Oxidation* (North-Holland, New York, 1976), Vol. 1, Chap. 10.
[2]N. F. Mott, Trans. Faraday Soc. **35**, 1175 (1939); **36**, 472 (1940).
[3]N. F. Mott, Trans. Faraday Soc. **43**, 429 (1947).
[4]N. Cabrera and N. F. Mott, Rep. Prog. Phys. **12**, 163 (1948-1949).
[5]R. Ghez, J. Chem. Phys. **58**, 1838 (1973).
[6]F. P. Fehlner, J. Electrochem. Soc. **131**, 1645 (1984).
[7]Maria Ronay and Peter Nordlander, Phys. Rev. B **35**, 9403 (1987).
[8]J. K. Nørskov and N. D. Lang, Phys. Rev. B **21**, 2131 (1981).
[9]B. Chakraborty, S. Holloway, and J. K. Nørskov, Surf. Sci. **152/153**, 660 (1985).
[10]P. Nordlander, S. Holloway, and J. K. Nørskov, Surf. Sci. **136**, 59 (1984).
[11]J. K. Nørskov, Phys. Rev. B **26**, 2875 (1982).
[12]P. Nordlander, J. K. Nørskov, and F. Besenbacher, J. Phys. F **16**, 1161 (1986).
[13]P. H. Dederichs and G. Leibfried, Phys. Rev. **188**, 1175 (1969).
[14]V. K. Tewary, Adv. Phys. **22**, 757 (1973).
[15]J. W. M. Frenken, J. F. van der Ween, and G. Allan, Phys. Rev. Lett. **51**, 1876 (1983).
[16]Maria Ronay (unpublished).
[17]R. I. Bickley, M. W. Roberts, and W. C. Storey, J. Chem. Soc. A **1971**, 2774 (1971).
[18]*Gmelins Handbuch der Anorganischen Chemie* (Verlag Chemie, Weinheim, 1973), System-Number 56, Teil B, p. 344.
[19]P. B. Sewell, D. F. Mitchell, and M. Cohen, Surf. Sci. **33**, 535 (1972).
[20]*Landolt-Börnstein* (Springer, Berlin, 1975), Vol. III/7b1, p. 541.
[21]A. Mukherjee and S. P. Wach, J. Less-Common Met. **92**, 289 (1983).